



## Single-step fluorescent probes to detect decrotonylation activity of HDACs through intramolecular reactions



Yusheng Xie <sup>a, b, 1</sup>, Liu Yang <sup>a, b, 1</sup>, Qingxin Chen <sup>a, b</sup>, Jie Zhang <sup>a, b</sup>, Ling Feng <sup>a, b</sup>, Jian Lin Chen <sup>c</sup>, Quan Hao <sup>d</sup>, Liang Zhang <sup>b, e</sup>, Hongyan Sun <sup>a, b, \*</sup>

<sup>a</sup> Department of Chemistry and COSDAF (Centre of Super-Diamond and Advanced Films), City University of Hong Kong, 83 Tat Chee Avenue, Kowloon, Hong Kong, China

<sup>b</sup> Shenzhen Research Institute of City University of Hong Kong, Shenzhen, 518057, China

<sup>c</sup> School of Science and Technology, The Open University of Hong Kong, Hong Kong Special Administrative Region

<sup>d</sup> School of Biomedical Sciences, University of Hong Kong, Hong Kong, China

<sup>e</sup> Department of Biomedical Science, College of Veterinary Medicine and Life Sciences, City University of Hong Kong, 83 Tat Chee Avenue, Kowloon, Hong Kong, China

### ARTICLE INFO

#### Article history:

Received 29 December 2019

Received in revised form

27 November 2020

Accepted 29 November 2020

Available online 30 December 2020

#### Keywords:

Single-step

Fluorescent probe

Decrotonylation

Histone deacetylases

Sirtuin

Intramolecular reaction

### ABSTRACT

Lysine crotonylation plays vital roles in gene transcription and cellular metabolism. Nevertheless, methods for dissecting the molecular mechanisms of decrotonylation remains limited. So far, there is no single-step fluorescent method developed for enzymatic decrotonylation activity detection. The major difficulty is that the aliphatic crotonylated lysine doesn't allow  $\pi$ -conjugation to a fluorophore and decrotonylation can not modulate the electronic state directly. Herein, we have designed and synthesized two activity-based single-step fluorogenic probes **KTcr-I** and **KTcr-II** for detecting enzymatic decrotonylation activity. These two probes can be recognized by histone deacetylases and undergo intramolecular nucleophilic exchange reaction to generate fluorescence signal. Notably, peptide sequence-dependent effect was observed. **KTcr-I** can be recognized by Sirt2 more effectively, while **KTcr-II** with LGKcr peptide sequence preferentially reacted with HDAC3. Compared to other methods of studying enzymatic decrotonylation activity, our single-step fluorescent method has a number of advantages, such as facileness, high sensitivity, cheap facility and little material consumed. We envision that the probes developed in this study will provide useful tools to screen inhibitors which suppress the decrotonylation activity of HDACs. Such probes will be useful for further delineating the roles of decrotonylation enzyme and aid in biomarker identification and drug discovery.

© 2020 Elsevier Masson SAS. All rights reserved.

## 1. Introduction

Increasing evidences have indicated that histone PTMs (post-translational modifications) are involved in various biological processes such as cell differentiation, gene transcription and organ-ismal development [1]. Lysine crotonylation (Kcr), an evolutionarily conserved PTM, was first identified in histone proteins in 2011 [2]. Recently, it has been proved that non-histone proteins can also undergo crotonylation [3]. Aberrant crotonylation of histones could

affect human health. Histone crotonylation specifically labels the potential enhancers and active gene promoters and stimulates transcription in mammalian cell genomes [2–4]. It has also been reported that crotonylation in histone affects kidney injury and is associated with cellular metabolism [5]. The enzymes responsible for removal of crotonylation are termed as “erasers” of Kcr.

Histone deacetylases (HDACs) are hydrolases that remove the acetyl groups from lysine residues in histones and other non-histone proteins [6]. HDACs are interesting therapeutic targets due to their important biological roles. To date, 18 distinct HDAC proteins have been identified in humans. Among them, Class I, II and IV utilize Zn as a cofactor, whereas Class III, also termed as sirtuins (Sirt1–7), shows a different mode of action by using NAD<sup>+</sup> as cofactor [6c]. Emerging evidence has demonstrated that HDACs can catalyze the removal of various alternative acyl groups of lysine

\* Corresponding author. Department of Chemistry and COSDAF (Centre of Super-Diamond and Advanced Films), City University of Hong Kong, 83 Tat Chee Avenue, Kowloon, Hong Kong, China.

E-mail address: [hongysun@cityu.edu.hk](mailto:hongysun@cityu.edu.hk) (H. Sun).

<sup>1</sup> These authors contributed equally to this work.

efficiently, such as succinyl, malonyl and crotonyl [7]. Until now, several HDACs, including Sirt2 and HDAC3, have been identified as “eraser” of Kcr [2,5b,7b,8]. Despite these advancements, our understanding of enzymes responsible for lysine decrotonylation and their inhibitor design remains limited.

To detect the decrotonylation activity of enzymes, several methods have been developed, including approaches that use Kcr antibody and HPLC [2,5b,7b,8]. However, antibody-based methods highly depend on the quality of the antibody used. HPLC approaches often need laborious preparation work and multistep protocols. Fluorescence detection for examining enzymatic activity has the advantage of high sensitivity and facileness [9]. In particular, fluorescence-based methods are useful for inhibitor screening because they can be performed in a high-throughput manner. Olsen et al. synthesized a fluorogenic probe for detecting decrotonylation activity of enzymes through two-step enzyme-coupled reactions [10]. However, this method needs an additional step of protease digestion. In addition, the aminomethylcoumarin (AMC) fluorophore needs to be conjugated to the neighbouring C-terminus of the acetylated lysine. This might not be ideal for enzyme recognition because of flanking effect [7b,11].

Till date, no single-step fluorescent method has been developed for enzymatic decrotonylation activity assay. It was noted that Buccella et al. has developed a peptide-based probe to detect decrotonylase activity, however, their detection method was based on absorbance readout [12]. The biggest challenge is that aliphatic crotonylated lysine does not allow  $\pi$ -conjugation to a fluorophore and decrotonylation is not able to modulate the electronic state directly [9b]. Previously, our group and others have developed several one-step fluorescent approaches for deacetylation/delipoylation activity detection based on intramolecular reactions [13]. We found that acylated lysine coupled with a NBD-conjugated and hydrophilic aminoethoxyl linker can be recognized by HDACs with moderate to good efficiency [13d-e]. We continued to explore whether the intramolecular reaction strategy can be applied to the design of single-step fluorescent probes to detect decrotonylation activity.

## 2. Results and discussion

### 2.1. Design and synthesis

In this study, we designed and synthesized two single-step activity-based fluorogenic probes (**KTcr-I**, lysine decrotonylation turn-on probe I and **KTcr-II**, lysine decrotonylation turn-on probe II, Scheme 1A) for enzymatic decrotonylation activity detection. The mechanism is based on a spontaneous intramolecular exchange reaction between non-fluorescent *O*-NBD and a free amine group which can be released by enzyme with decrotonylation activity (Scheme 1A). The yielded product *N*-NBD is highly fluorescent. In addition, the difference between **KTcr-I** and **KTcr-II** is the peptide sequence incorporated in **KTcr-II** due to the sequence-dependent effect for Kcr recognition.

The synthetic route for **KTcr-I** was illustrated as scheme 1B. The synthesis started with Boc-Lys-OH, which is readily available from commercial vendors. Selective protection is then performed with Fmoc at  $\epsilon$ -amino group of lysine side chain, followed by coupling with a flexible and hydrophilic aminoethoxyl linker. Further deprotection of Fmoc was subsequently carried out to afford compound **3** with 75% yield. The use of crotonic anhydride to functionalize the free amino group generated intermediate **4**. The final step was accomplished by nucleophilic substitution of NBD-F under basic condition to generate the probe **KTcr-I**. The approach to obtain probe **KTcr-II** (Scheme 1B) is slightly different. An Ac-Leu-Gly-OH (compound **7**) building block was first synthesized by

standard solid-phase peptide synthesis with 52% overall yield [14]. Intermediate **4** was treated with TFA to give compound **8** with a quantitative yield. **8** underwent coupling reaction with peptide building block **7** in the presence of the activator of HOBt/HBTU to yield **9**, which was subjected to substitution with NBD-F to afford the desired probe **KTcr-II**. The final compound **KTcr-I** and **KTcr-II** were both confirmed by NMR and mass spectrometry.

### 2.2. Fluorescence turn-on molecular mechanism studies

With the probes in hand, we first carried out the HPLC studies to evaluate whether crotonylated lysine in the probe can be recognized by sirtuins. **KTcr-I** was used as the representative probe. Briefly, 40  $\mu$ M **KTcr-I** was incubated with Sirt2 and cofactor  $\text{NAD}^+$  in HEPES buffer (pH 8.0) at 37 °C. After 3 h of reaction, the enzymatic reaction was quenched by methanol and aliquot was analyzed by HPLC. HPLC analysis showed the appearance of a new peak after reaction (Peak 2, retention time: 22.5 min, Fig. 1A). Furthermore, the eluted fraction collected from this peak showed the expected mass value of the decrotonylated/exchanged product (Fig. 1B). Nevertheless, no product was observed in control experiments, including samples without addition of  $\text{NAD}^+$  or/and enzyme (Fig. 1A and Fig. S1). These data indicated that 1) the probe can be recognized by the known Kcr “eraser” sirtuin2, 2) the intramolecular exchange reaction between *O*-NBD and amine occurred.

### 2.3. Absorbance and fluorescence analysis

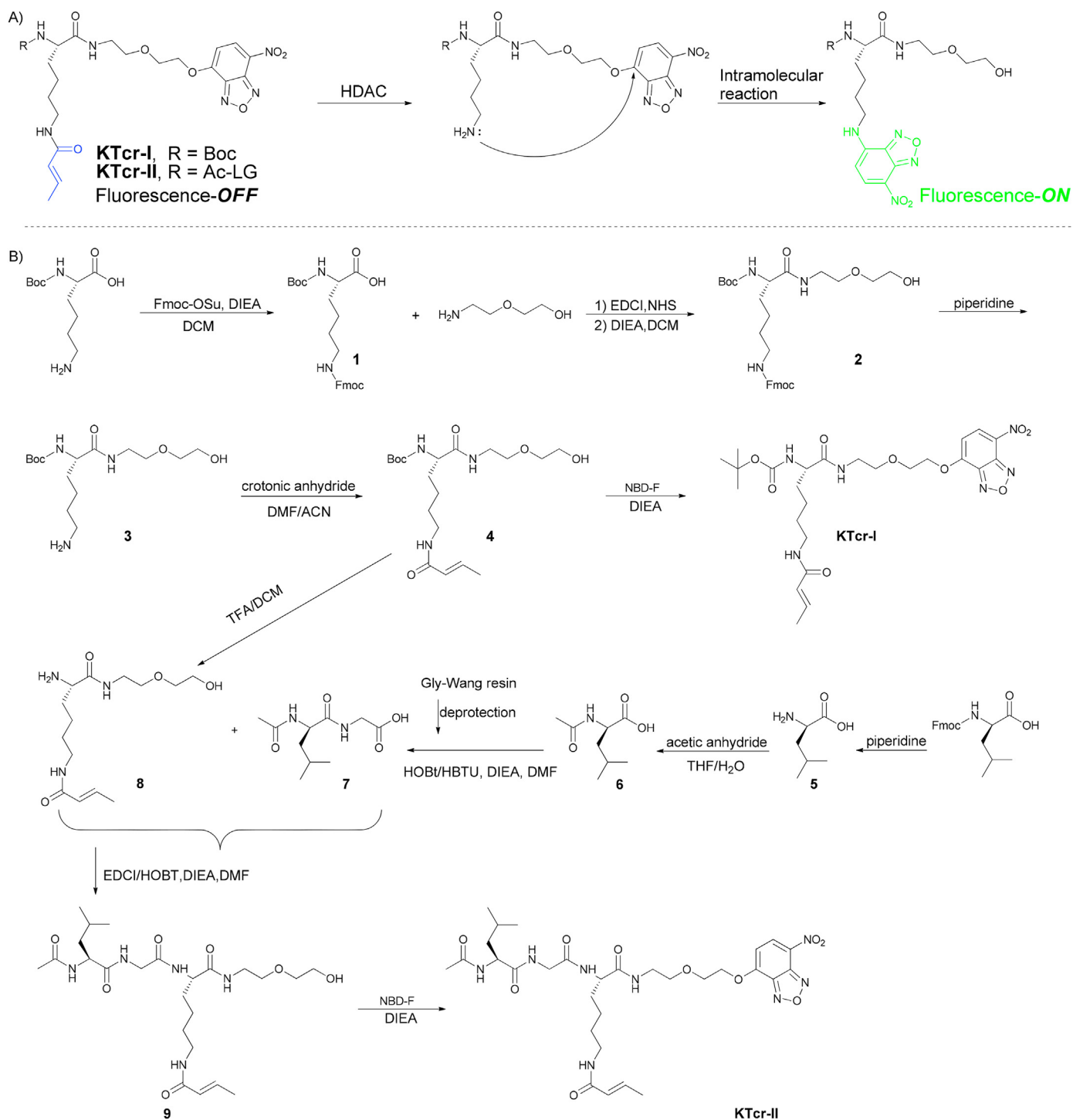
Next, we performed detailed absorbance and fluorescence analysis with **KTcr-I**. The absorbance spectra were recorded before and after enzymatic reaction (Fig. 2A). At the beginning, an obvious absorption peak at 380 nm, which corresponds to that of *O*-NBD group, was observed with **KTcr-I**. After enzymatic reaction with Sirt2 and  $\text{NAD}^+$ , a new absorption peak was detected at 480 nm, indicating the formation of *N*-NBD. Some absorbance at 380 nm was observed after enzymatic reaction. This is due to incomplete reaction of enzymatic decrotonylation, which is consistent with our HPLC analysis. The results also agree well with the reported literature that the decrotonylation activity of Sirt2 is much lower than its deacetylation activity [7b]. Subsequently, more detailed fluorescence studies were carried out (Fig. 2B). Results showed that **KTcr-I** only, and **KTcr-I** in the presence of Sirt2 or  $\text{NAD}^+$  displayed negligible fluorescence ( $\lambda_{\text{ex}} = 480$  nm). However, a strong emission peak was observed upon addition of Sirt2 and  $\text{NAD}^+$ . The fluorescence increase was determined to be around 5-fold.

### 2.4. Time-dependent experiments

Following that time-dependent enzymatic reaction with Sirt2 was conducted by fluorescence analysis. The fluorescence spectra of the probe under enzymatic condition were periodically recorded (Fig. 3A). Initially, the fluorescence intensity of the probe was weak and increased progressively during incubation. It plateaued after 3 h. Those data together unambiguously confirmed that the reaction was catalysed by enzymatic activity rather than environmental factors.

### 2.5. Inhibition experiments

We next investigated the capability of probe **KTcr-I** to evaluate the potency of Sirt2 inhibitors by exposing Sirt2 to a known inhibitor, tenovin-6. Increasing concentrations (0, 2, 4, 10, 20, 40, 80, 120, 160  $\mu$ M) of inhibitor was firstly added to Sirt2 (40 ng/ $\mu$ l) in HEPES buffer and incubated at 37 °C for 30 min. **KTcr-I** (10  $\mu$ M) was



**Scheme 1.** (A) Mechanism of our strategy to detect enzymatic decrotonylation by single-step fluorescent method. (B) Synthetic route of probe **KTcr-I** and **KTcr-II**.

then added and incubated for another 3 h. Subsequently, the fluorescence of the reaction samples was measured respectively. The percentage of the total activity of Sirt2 was calculated from the fluorescence intensity of samples at 545 nm relative to the positive control (without tenovin-6). The  $IC_{50}$  value for Sirt2 was determined to be 33.99  $\mu$ M by calculating from the plot of enzyme activity and the log concentration of tenovin-6 (Fig. 3B). These data indicated that probe **KTcr-I** can provide useful tool to screen potential inhibitors of decrotonylation enzymes.

## 2.6. Selectivity studies

We then moved on to study the response of the designed fluorescent probes using a series of HDACs (Fig. 4), including Sirt1-3, 5, 6 and HDAC3. The sequence-dependent effect of sirtuins recognition toward various substrates prompted us to include **KTcr-II**, which contains a peptide fragment (LGKcr, Scheme 1A) [7b,10]. Our results indicated that Sirt1 and Sirt2 showed decrotonylation activity, which are in agreement with the previous literature [7b].

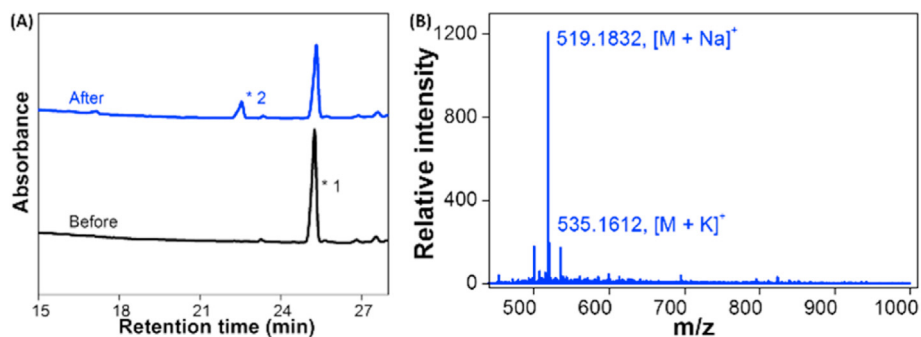


**Fig. 1.** (A) HPLC analysis of the enzymatic reaction of **KTcr-I** (40  $\mu\text{M}$ ) with recombinant Sirt2 (100 ng/ $\mu\text{l}$ ) in HEPES buffer (20 mM, pH = 8.0) with 200  $\mu\text{M}$  NAD<sup>+</sup> at 37  $^{\circ}\text{C}$  for 3 h. The retention time of peak 1 and 2 was 25.3 and 22.5 min respectively. (B) ESI mass spectrum of the peak at 22.5 min in LC. The mass peak corresponds to the tandem deacetylated and exchanged product.

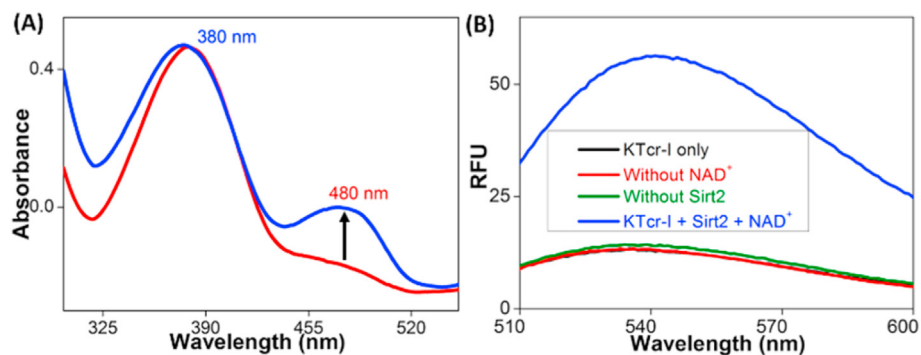


**Fig. 2.** (A) Absorption spectra of **KTcr-I** (10  $\mu\text{M}$ , prepared from 5 mM stock in DMSO) before and after enzymatic reaction with Sirt2 (40 ng/ $\mu\text{l}$ ) in HEPES buffer (20 mM, pH = 8.0) with 200  $\mu\text{M}$  NAD<sup>+</sup> at 37  $^{\circ}\text{C}$  for 3 h. (B) Fluorescence spectra of **KTcr-I** (10  $\mu\text{M}$ , prepared from 5 mM stock in DMSO) with Sirt2 (40 ng/ $\mu\text{l}$ ) under various conditions ( $\lambda_{\text{ex}} = 480$  nm) for 3 h.

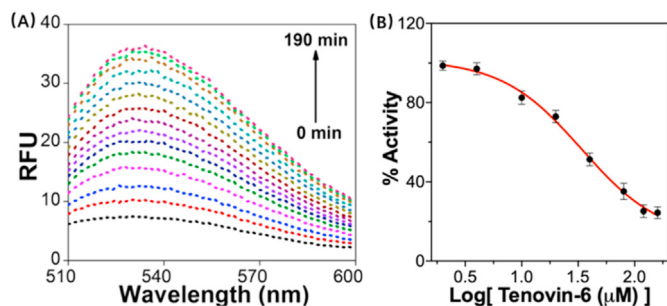


**Fig. 3.** (A) Time dependent study of **KTcr-I** (10  $\mu\text{M}$ , prepared from 5 mM stock in DMSO) incubated with Sirt2 (40 ng/ $\mu\text{l}$ ) in HEPES buffer (20 mM, pH = 8.0) with 200  $\mu\text{M}$  NAD<sup>+</sup> at 37  $^{\circ}\text{C}$  ( $\lambda_{\text{ex}} = 480$  nm). (B) Dose-response inhibition curve of Sirt2 deacetylation activity by Tenovin-6 using **KTcr-I** (10  $\mu\text{M}$ ). Values of Y axis correspond to the average enzyme activity of three independent experiments.

Sirt5 and Sirt6 did not show any activity toward both probes because Sirt5 was reported to recognize Ksuc and Kmal and Sirt6 can remove long-chain fatty acid group preferably [7a,15]. The activity of Sirt3 was not observed, indicating that the crotonylated lysine of probe **KTcr-I** and **KTcr-II** might not be a good substrate for Sirt3. Importantly, peptide-sequence dependent effect of sirtuins' deacetylation activity was observed by careful comparison of the enzymatic data of the two probes. Sirt2 is known to possess a large hydrophobic active pocket and it can accommodate many acyl groups such as acetyl, propionyl, butyryl, octanoyl, myristoyl and crotonyl [16]. The newly designed probes **KTcr-I/II** showed that one single crotonylated lysine in probes can be recognized by Sirt2 with a moderate to high efficiency. Specifically, probe **KTcr-I**

showed preference of Sirt2 over other HDACs. It is noted that **KTcr-II** showed mediocre solubility because of hydrophobic amino acid residues. Nevertheless, the probe **KTcr-II** was recognized by HDAC3 preferably compared with other sirtuins. This is consistent with Olsen's work [10]. In addition, we tested the selectivity of **KTcr-I** with other potential interferents, including butylamine and various amino acids. 10  $\mu\text{M}$  **KTcr-I** was treated with different species (100  $\mu\text{M}$ ), and the fluorescent spectra of reaction mixtures were recorded respectively (Fig. S2). The results indicated that all the tested species, including lysine, histidine and cysteine, only induced negligible fluorescence increment. The substantial fluorescence enhancement caused only by Sirt2 unambiguously proved that the turn-on fluorescence comes from the intramolecular nucleophilic exchange reaction upon enzymatic deacetylation reaction. Those experiments together proved that the current panel of probes (**KTcr-I** and **KTcr-II**) are suitable for deacetylation activity detection.

### 3. Conclusions

In conclusion, we have developed two single-step fluorescent probes (**KTcr-I** and **KTcr-II**) to detect deacetylation activity of HDACs. The probes can be recognized by HDACs and undergo intramolecular nucleophilic exchange reaction to generate fluorescence signal. Notably, peptide sequence-dependent effect was observed. **KTcr-I** can be recognized by Sirt2 more efficiently, while **KTcr-II** with LGKcr short sequence preferentially reacts with HDAC3. Compared with other methods such as two-step fluorescent method to detect enzymatic deacetylation activity, our single-step fluorescent method is more facile and sensitive, and it allows real-time monitoring the deacetylation activity. We

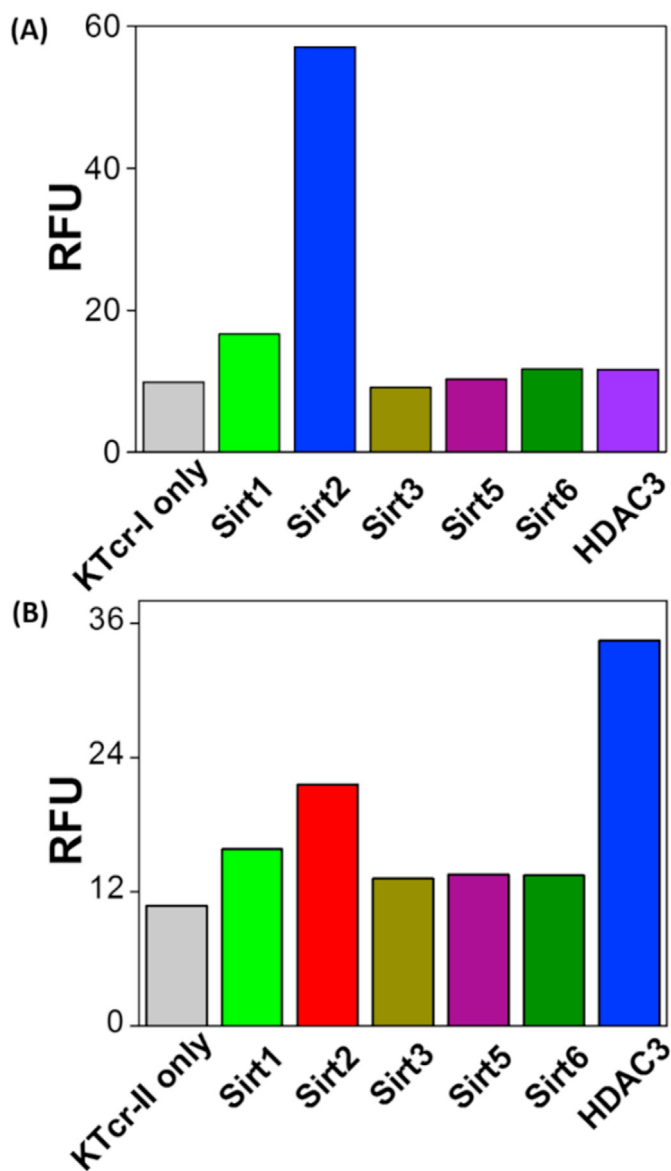


Fig. 4. (A) Fluorescence detection of **KTCr-I** with different HDACs. (B) Fluorescence detection of **KTCr-II** with different HDACs. Reaction condition: probe, 10  $\mu$ M (10  $\mu$ M, prepared from 5 mM stock in DMSO); HDACs, 40 ng/ $\mu$ l;  $\lambda_{ex}$  = 480 nm;  $\lambda_{em}$  = 545 nm in HEPES buffer (20 mM, pH = 8.0).

envision that the probes will provide useful tools for further delineating the roles of deacetylation enzymes in biology.

## 4. Experimental section

### 4.1. Materials and instruments

Starting materials were obtained from commercial vendors and used directly. The anhydrous solvents used were purchased from J&K company or produced as common procedures. To monitor organic reactions, thin layer chromatography (TLC) analysis by UV or ninhydrin stain visualization were conducted using pre-coated silica plates (Merck 60 F254 nm, 250  $\mu$ m thickness). Compound purification was performed by flash column chromatography using silica gel (Merck 60 F254 nm, 70–200 mesh).  $^1\text{H}$  NMR,  $^{13}\text{C}$  NMR spectra were analyzed with Bruker 300 MHz/400 MHz NMR spectrometers. Data are reported with chemical shift values in ppm

by using the corresponding solvent peaks as reference ( $^1\text{H}$ ,  $\text{CD}_3\text{OD}$  = 3.31 ppm,  $\text{CDCl}_3$  = 7.26 ppm,  $\text{CD}_3\text{CN}$  = 1.94 ppm;  $^{13}\text{C}$ ,  $\text{CD}_3\text{OD}$  = 49.00 ppm,  $\text{CDCl}_3$  = 77.16 ppm,  $\text{CD}_3\text{CN}$  = 1.32, 118.26 ppm). Multiplicities are indicated as follows: m (multiplet), dd (doublet of doublets), br (broad singlet), q (quartet), t (triplet), d (doublet), s (singlet). To obtain mass spectra, a PC Sciex API 150 EX ESI-mass spectrometer was used.

pH value was measured with a HANNA HI 2211 pH/ORP meter. To carry out analytical high-performance liquid chromatography (HPLC) analysis, a Waters 2489 UV/Visible Detector and Waters 1525 Binary HPLC Pump were used. A reverse-phase Phenomenex Luna $\text{\textcircled{R}}$  Omega 5  $\mu$ m Polar C18 100  $\text{\AA}$  250  $\times$  4.6 mm column was utilized for separation analysis. Acetonitrile and water were used as eluents with the flow rate of 1 ml/min. Fluorescence detection was conducted using a FluoroMax-4 fluorescence photometer. Absorption analysis was performed with UV-VS shimadzu 1700. Sirt1/2/3/5/6 in this study were recombinantly expressed and purified as previously reported [17]. HDAC3/NCOR1 was purchased from Enzo Lifescience.

### 4.2. Enzymatic reaction

The probe **KTCr-I** or **KTCr-II** was incubated with sirtuin and cofactor  $\text{NAD}^+$  for specified time at 37  $^\circ\text{C}$  in 20 mM HEPES buffer (pH = 8.0) with 1 mM  $\text{MgCl}_2$ , 2.7 mM KCl and 150 mM NaCl.

### 4.3. Enzymatic reaction monitoring with LC-MS using probe **KTCr-I**

A total reaction volume of 50  $\mu$ l was used for enzymatic reaction. After specific reaction time, the enzymatic reactions were quenched by addition of methanol (250  $\mu$ l), vortexed and spun-down. Supernatant was collected and applied for reversed HPLC analysis. Water and acetonitrile were used as the mobile phase with a flow rate (1 ml/min). The newly generated peak was collected for ESI-MS analysis directly.

### 4.4. Measurement of absorption and fluorescence spectra of probes **KTCr-I** and **KTCr-II**

A total reaction volume of 50  $\mu$ l was set for the reaction. When the reaction was complete, absorption and fluorescence spectra were measured. The absorbance spectra were collected between 300 and 550 nm. The fluorescence spectra were collected between 510 and 600 nm with excitation wavelength of 480 nm and slit width of 5 nm.

### 4.5. 6-(((9H-fluoren-9-yl)methoxy)carbonyl)amino)-2-((tert-butoxycarbonyl)amino)hexanoic acid (**1**)

*N,N*-Diisopropylethylamine (DIEA, 517 mg, 4 mmol) was added to the solution of Fmoc *N*-hydroxysuccinimide ester (607 mg, 1.8 mmol) and *N $\alpha$ -(*tert*-Butoxycarbonyl)-lysine (493 mg, 2 mmol) in anhydrous dichloromethane, and the reaction was performed overnight at room temperature. After completion of the reaction and solvent removal under vacuo, the residue was purified by flash chromatography (EA/MeOH, 100/1) to afford the product **1** as a light-yellow liquid (413 mg, 49% yield).  $^1\text{H}$  NMR (DMSO, 400 MHz) (ppm): 12.41 (s, 1H), 7.89 (d,  $J$  = 8.0 Hz, 2H), 7.68 (d,  $J$  = 8.0 Hz, 2H), 7.41 (t,  $J$  = 8.0 Hz, 2H), 7.33 (t,  $J$  = 8.0 Hz, 2H), 7.28 (t,  $J$  = 4.0 Hz, 1H), 7.04 (d,  $J$  = 8.0 Hz, 1H), 4.29 (d,  $J$  = 8.0 Hz, 2H), 4.20 (t,  $J$  = 8.0 Hz, 1H), 3.84–3.79 (m, 1H), 2.97–2.93 (m, 2H), 1.66–1.37 (m, 15H).  $^{13}\text{C}$  NMR (DMSO, 100 MHz) (ppm): 174.7, 156.5, 156.1, 144.4, 141.2, 128.1, 127.5, 125.6, 120.6, 78.4, 65.6, 60.2, 47.2, 31.2, 30.9, 29.4, 28.7, 23.4. ESI-MS calcd for  $[\text{M} - \text{H}]^-$  467.23; Found 467.60.*

4.6. (9H-fluoren-9-yl)methyl tert-butyl (6-((2-(2-hydroxyethoxy)ethyl)amino)-6-oxohexane-1,5-diyl)dicarbamate (**2**)

*N*-(3-Dimethylaminopropyl)-*N'*-ethylcarbodiimide hydrochloride (230 mg, 1.2 mmol) and *N*-Hydroxysuccinimide (127 mg, 1.1 mmol) were added to a solution of **1** (413 mg, 0.88 mmol) in anhydrous dichloromethane (2 ml), and the reaction was performed for 2 h at room temperature. *N*, *N*-Diisopropylethylamine (336 mg, 2.6 mmol) and 2-(2-Aminoethoxy)ethanol (116 mg, 1.1 mmol) were then added, and the mixture was reacted overnight furtherly. The solvent was removed under vacuo, the residue was purified by flash chromatography (DCM/MeOH, 50/1) to afford the product **2** as a colorless liquid (254 mg, 52% yield). <sup>1</sup>H NMR (CD<sub>3</sub>OD, 400 MHz) (ppm): 7.78 (d, *J* = 8.0 Hz, 2H), 7.63 (d, *J* = 8.0 Hz, 2H), 7.38 (t, *J* = 8.0 Hz, 2H), 7.30 (t, *J* = 8.0 Hz, 2H), 4.33 (d, *J* = 8.0 Hz, 2H), 4.17 (t, *J* = 8.0 Hz, 1H), 3.99–3.98 (m, 1H), 3.64 (t, *J* = 4.0 Hz, 2H), 3.55–3.47 (m, 4H), 3.37 (t, *J* = 4.0 Hz, 2H), 3.12–3.08 (m, 2H), 1.73–1.42 (m, 15H). <sup>13</sup>C NMR (CD<sub>3</sub>OD, 100 MHz) (ppm): 175.4, 159.0, 157.9, 145.4, 142.7, 128.8, 128.2, 126.2, 121.0, 80.7, 73.5, 70.6, 67.7, 62.3, 56.2, 41.5, 40.4, 33.2, 30.9, 30.6, 28.8, 24.1. ESI-MS calcd for [M+Na]<sup>+</sup> 578.29; Found 578.6.

4.7. tert-butyl (6-amino-1-((2-(2-hydroxyethoxy)ethyl)amino)-1-oxohexan-2-yl)carbamate (**3**)

A solution of **2** (254 mg, 0.46 mmol) in piperidine/DCM (1:1, 1 ml) was reacted at room temperature and monitored with TLC. After completion of the reaction, cold ethyl ether was added to wash the reaction residues and obtained the product **3** as a light yellow oil (114 mg, 75% yield). <sup>1</sup>H NMR (CD<sub>3</sub> OD, 400 MHz) δ (ppm): 4.02–3.94 (m, 1H), 3.63 (t, *J* = 4.0 Hz, 2H), 3.50 (t, *J* = 4.0 Hz, 4H), 3.38–3.32 (m, 2H), 2.91 (t, *J* = 4.0 Hz, 2H), 1.71–1.53 (m, 6H), 1.40 (s, 9H). ESI-MS calcd for [M+H]<sup>+</sup> 334.23; Found 334.6.

4.8. (*E*)-tert-butyl (6-(but-2-enamido)-1-((2-(2-hydroxyethoxy)ethyl)amino)-1-oxohexan-2-yl)carbamate (**4**)

**3** (83 mg, 0.25 mmol) was dissolved in DMF/acetonitrile mixture (1:3, 1.2 ml) in ice-bath. To this solution was added crotonic anhydride (50 mg, 0.32 mmol) slowly. After completion of the reaction and removal of the solvents, the crude product was purified with column chromatography (DCM/MeOH, 100/1–30/1) to yield **4** (49 mg, 49% yield). <sup>1</sup>H NMR (CD<sub>3</sub> OD, 400 MHz) δ (ppm): 6.80–6.70 (m, *J*<sub>1</sub> = 4.0 Hz, *J*<sub>2</sub> = 16.0 Hz, 1H), 5.91 (d, *J* = 16.0 Hz, 1H), 4.02–3.94 (m, 1H), 3.65 (t, *J* = 4.0 Hz, 2H), 3.52 (t, *J* = 4.0 Hz, 4H), 3.42–3.35 (m, 2H), 3.21 (t, *J* = 4.0 Hz, 2H), 1.83 (d, *J* = 4.0 Hz, 3H), 1.76–1.43 (m, 15H). <sup>13</sup>C NMR (CD<sub>3</sub>OD, 100 MHz) (ppm): 175.3, 168.6, 157.8, 140.6, 126.2, 80.6, 73.5, 70.5, 62.3, 56.1, 40.4, 40.1, 33.2, 30.2, 28.8, 24.3, 17.9. ESI-MS calcd for [M+Na]<sup>+</sup> 424.25; Found 424.5.

4.9. (*E*)-tert-butyl (6-(but-2-enamido)-1-((2-(2-((7-nitrobenzo[*c*][1,2,5]oxadiazol-4-yl)oxy)ethoxy)ethyl)amino)-1-oxohexan-2-yl)carbamate (**KTcr-I**)

NBD-F (29 mg, 0.16 mmol) and *N*, *N*-Diisopropylethylamine (40 mg, 0.31 mmol) were added to a solution of **4** (49 mg, 0.12 mmol) in anhydrous DCM/DMF (3:1). The mixture was stirred overnight at room temperature. After completion of the reaction and solvent removal under reduced vacuo, the residue was purified by flash column chromatography (DCM/MeOH, 50/1–20/1), followed by preparative TLC, to afford the product **KTcr-I** as a yellow solid (16 mg, 24% yield). <sup>1</sup>H NMR (CD<sub>3</sub> OD, 400 MHz) δ (ppm): 8.64 (d, *J* = 8.0 Hz, 1H), 6.99 (d, *J* = 8.0 Hz, 1H), 6.77–6.67 (m, *J*<sub>1</sub> = 8.0 Hz, *J*<sub>2</sub> = 16.0 Hz, 1H), 5.88 (d, *J* = 16.0 Hz, 1H), 4.57 (t, *J* = 4.0 Hz, 2H), 3.98–3.94 (m, 3H), 3.65 (t, *J* = 4.0 Hz, 2H), 3.49–3.33 (m, 2H), 3.17

(t, *J* = 4.0 Hz, 2H), 1.83 (d, *J* = 8.0 Hz, 3H), 1.74–1.40 (m, 15H). <sup>13</sup>C NMR (CD<sub>3</sub>OD, 100 MHz) (ppm): 175.5, 168.7, 157.8, 155.9, 146.9, 145.6, 140.7, 136.2, 131.0, 126.2, 106.8, 80.6, 71.8, 71.0, 69.9, 56.2, 40.4, 40.0, 33.2, 30.1, 28.8, 24.3, 17.8. HRMS calcd for [M+Na]<sup>+</sup> 587.2441; Found 587.2428.

4.10. 2-amino-4-methylpentanoic acid (**5**)

A solution of Fmoc-Leu-OH (3 g, 8.5 mmol) in 20% piperidine in DMF was reacted at room temperature for 1 h and monitored with TLC. After reaction finish, cold ethyl ether was added to wash the reaction residues and obtained the pure product **5** (1.1 g, 100% yield). <sup>1</sup>H NMR (CD<sub>3</sub> OD, 400 MHz) δ (ppm): 3.54–3.51 (m, 1H), 1.79–1.75 (m, 2H), 1.65–1.58 (q, *J* = 8.0 Hz, 1H), 0.98 (t, *J* = 8.0 Hz, 6H). ESI-MS calcd for [M+Na]<sup>+</sup> 154.09; Found 154.3.

4.11. 2-acetamido-4-methylpentanoic acid (**6**)

To a solution of Leu-OH (**5**, 1.1 g, 8.5 mmol) in 70% THF/H<sub>2</sub>O (80 ml) was added acetic anhydride dropwise and slowly in ice-batch. The mixtures were monitored with TLC. After reaction finish, the volatile was removed to obtain the pure product **6** in a quantitative yield. <sup>1</sup>H NMR (DMSO, 400 MHz) δ (ppm): 12.48 (br, 1H), 8.09 (d, *J* = 8.0 Hz, 1H), 4.21–4.16 (m, 1H), 1.83 (s, 3H), 1.67–1.57 (m, 1H), 1.50–1.47 (m, 2H), 0.89–0.83 (m, 6H). <sup>13</sup>C NMR (DMSO, 100 MHz) (ppm): 174.3, 169.2, 50.1, 24.3, 22.8, 22.3, 21.3. ESI-MS calcd for [M – H]<sup>-</sup> 172.11; Found 172.10.

4.12. 2-(2-(acetamido-4-methylpentanamido)acetic acid (**7**)

It was synthesized on a 0.5 mmol scale Fmoc-Gly-Wang resin (capacity, 0.41 mmol/g). To the swelled and pre-deprotected Gly-Wang resin in DMF were added 2-(1*H*-benzotriazole-1-yl)-1,3,3-tetramethyluroniumhexafluorophosphate (HBTU, 948 mg, 2.5 mmol), 1-Hydroxybenzotriazole hydrate (HOBT, 338 mg, 2.5 mmol), **6** (433 mg, 2.5 mmol) and *N*, *N*-Diisopropylethylamine (DIEA, 646 mg, 5 mmol). The mixtures were reacted for 2 h, followed by cleavage by trifluoroacetic acid, precipitation in ethyl ether to obtain the crude peptide. With further purification by preparative HPLC, the pure product **7** was obtained (60 mg, 52% yield). <sup>1</sup>H NMR (CD<sub>3</sub> OD, 400 MHz) δ (ppm): 4.44–4.41 (m, 1H), 3.95–3.82 (m, 2H), 1.98 (s, 3H), 1.70–1.65 (m, 1H), 1.63–1.53 (m, 2H), 0.96–0.91 (m, 6H). ESI-MS calcd for [M – H]<sup>-</sup> 229.13; Found 229.2.

4.13. 2-amino-6-(but-2-enamido)-*N*-(2-(2-hydroxyethoxy)ethyl)hexanamide (**8**)

A solution of **4** (70 mg, 0.17 mmol) in trifluoroacetic acid/DCM (1:1) was reacted at room temperature and monitored with TLC. After reaction finish, cold ethyl ether was added to wash the reaction residues two times and the pure product **8** was obtained in quantitative yield. <sup>1</sup>H NMR (CD<sub>3</sub> OD, 400 MHz) δ (ppm): 6.81–6.72 (m, *J*<sub>1</sub> = 8.0 Hz, *J*<sub>2</sub> = 16.0 Hz, 1H), 5.92 (d, *J* = 16.0 Hz, 1H), 4.52–4.50 (m, 1H), 3.85–3.75 (m, 2H), 3.68–3.52 (m, 4H), 3.46–3.37 (m, 2H), 3.23 (t, *J* = 8.0 Hz, 2H), 1.83 (m, *J* = 8.0 Hz, 5H), 1.59–1.52 (m, 2H), 1.44–1.37 (m, 2H). ESI-MS calcd for [M+H]<sup>+</sup> 302.20; Found 302.60.

4.14. 2-(2-(2-(acetamido-4-methylpentanamido)acetamido)-6-((*E*)-but-2-enamido)-*N*-(2-(2-hydroxyethoxy)ethyl)hexanamide (**9**)

1-Hydroxybenzotriazole hydrate (HOBT, 18 mg, 0.13 mmol) and *N*-(3-Dimethylaminopropyl)-*N'*-ethylcarbodiimide hydrochloride (EDCI, 25 mg, 0.13 mmol) were added to a solution of compound **7** (22 mg, 0.1 mmol) in anhydrous DMF (0.5 ml), and the mixture was

stirred for 1.5 h at room temperature. After activation, **8** (33 mg, 0.11 mmol) and *N,N*-Diisopropylethylamine (DIEA, 39 mg, 0.3 mmol) were then added, and the residues were stirred overnight furtherly. After completion of the reaction and solvent removal under vacuo, the residue was purified by flash chromatography (DCM/MeOH, 30/1–10/1) to afford the product **9** (27 mg, 53% yield). <sup>1</sup>H NMR (CD<sub>3</sub> OD, 400 MHz) δ (ppm): 6.87–6.78 (m, *J*<sub>1</sub> = 16.0 Hz, *J*<sub>2</sub> = 4.0 Hz, 1H), 6.03 (d, *J* = 16.0 Hz, 1H), 4.39–4.30 (m, 2H), 4.02–3.90 (m, 2H), 3.73 (t, *J* = 4.0 Hz, 2H), 3.61 (t, *J* = 4.0 Hz, 4H), 3.47 (t, *J* = 4.0 Hz, 2H), 3.40–3.37 (m, 2H), 2.08 (s, 3H), 1.92 (d, *J* = 4.0 Hz, 3H), 1.84–1.75 (m, 2H), 1.70–1.67 (m, 2H), 1.64–1.58 (m, 2H), 1.42–1.38 (m, 3H), 1.06–1.0 (m, 6H). ESI-MS calcd for [M+Na]<sup>+</sup> 536.32; Found 536.6.

#### 4.15. 2-(2-(2-acetamido-4-methylpentanamido)acetamido)-6-((*E*)-but-2-enamido)-*N*-(2-(2-((7-nitrobenzo[*c*]1,2,5-oxadiazol-4-yl)oxy)ethoxy)ethyl) hexanamide (**KTcr-II**)

*N,N*-Diisopropylethylamine (21 mg, 0.16 mmol) and NBD-F (15 mg, 0.08 mmol) were added to a solution of **9** (27 mg, 0.05 mmol) in anhydrous DCM/DMF (3:1). The reaction was performed overnight at room temperature. After solvent removal under reduced vacuo, the residue was purified by flash column chromatography (DCM/MeOH, 50/1–20/1), followed by preparative HPLC, to afford the product **KTcr-II** as a yellow solid (2 mg, 6% yield). <sup>1</sup>H NMR (CD<sub>3</sub> OD, 300 MHz) δ (ppm): 8.64 (d, *J* = 8.0 Hz, 1H), 6.99 (m, *J* = 8.0 Hz, 1H), 6.79–6.67 (m, *J*<sub>1</sub> = 4.0 Hz, *J*<sub>2</sub> = 20.0 Hz, 1H), 5.90 (d, *J* = 20.0 Hz, 1H), 4.58 (t, *J* = 4.0 Hz, 2H), 4.28–4.20 (m, 2H), 3.97 (t, *J* = 4.0 Hz, 2H), 3.92–3.74 (m, 2H), 3.67–3.63 (m, 2H), 3.46–3.34 (m, 2H), 3.21–3.15 (m, 2H), 1.98 (d, *J* = 4.0 Hz, 3H), 1.84–1.81 (m, *J* = 4.0 Hz, 3H), 1.78–1.63 (m, 3H), 1.62–1.55 (m, 2H), 1.50–1.42 (m, 2H), 1.40–1.28 (m, 2H), 0.97–0.90 (m, 6H). <sup>13</sup>C NMR (CD<sub>3</sub>OD, 75 MHz) (ppm): 176.1, 174.5, 174.1, 171.8, 168.7, 156.1, 147.0, 145.6, 140.7, 136.3, 131.0, 126.2, 106.9, 72.0, 70.8, 69.9, 55.0, 54.2, 43.9, 41.5, 40.6, 40.1, 32.6, 30.0, 26.0, 24.4, 23.4, 22.6, 22.1, 17.9. HRMS calcd for [M+Na]<sup>+</sup> 699.3078; Found 699.3066.

#### Declaration of competing interest

The authors declare that they have no known competing financial interests or personal relationships that could have appeared to influence the work reported in this paper.

#### Acknowledgments

This work was supported by the Science Technology and Innovation Committee of Shenzhen Municipality (JCYJ20180507181654823, JCYJ20170413141047772), the National Natural Science Foundation of China (21778044) and Sichuan Science and Technology Program (2018JY0360).

#### Appendix A. Supplementary data

Supplementary data to this article can be found online at <https://doi.org/10.1016/j.ejmech.2020.113120>.

#### References

- [1] (a) M. Berdasco, M. Esteller, *Dev. Cell* 19 (2010) 698; (b) J. Füllgrabe, E. Kavanagh, B. Joseph, *Oncogene* 30 (2011) 3391; (c) H. Huang, S. Lin, B.A. Garcia, Y. Zhao, *Chem. Rev.* 115 (2015) 2376.
- [2] M. Tan, H. Luo, S. Lee, F. Jin, J.S. Yang, E. Montellier, T. Buchou, Z. Cheng, S. Rousseaux, N. Rajagopal, Z. Lu, Z. Ye, Q. Zhu, J. Wysocka, Y. Ye, S. Khochbin, B. Ren, Y. Zhao, *Cell* 146 (2011) 1016.
- [3] W. Xu, J. Wan, J. Zhan, X. Li, H. He, Z. Shi, H. Zhang, *Cell Res.* 27 (2017) 946.
- [4] S.K. Kota, R. Feil, *Dev. Cell* 19 (2010) 675.
- [5] (a) O. Ruiz-Andres, M.D. Sanchez-Niño, P. Cannata-Ortiz, M. Ruiz-Ortega, J. Egido, A. Ortiz, A.B. Sanz, *Dis. Models & Mech.* 9 (2016) 633; (b) R. Fellows, J. Denizot, C. Stellato, A. Cuomo, P. Jain, E. Stoyanova, S. Balázs, Z. Hajnád, A. Liebert, J. Kazakevych, H. Blackburn, R.O. Corrêa, J.L. Fachi, F.T. Sato, W.R. Ribeiro, C.M. Ferreira, H. Perée, M. Spagnuolo, R. Mattiuz, C. Matolcsi, J. Guedes, J. Clark, M. Veldhoen, T. Bonaldi, M.A.R. Vinolo, P. Varga-Weisz, *Nat. Commun.* 9 (2018) 105.
- [6] (a) A.P. Wolffe, *Science* 272 (1996) 371; (b) D.D. Leipe, D. Landsman, *Nucleic Acids Res.* 25 (1997) 3693; (c) R.H. Houtkooper, E. Pirinen, J. Auwerx, *Nat. Rev. Mol. Cell Biol.* 13 (2012) 225.
- [7] (a) J. Du, Y. Zhou, X. Su, J.J. Yu, S. Khan, H. Jiang, J. Kim, J. Woo, J.H. Kim, B.H. Choi, B. He, W. Chen, S. Zhang, R.A. Cerione, J. Auwerx, Q. Hao, H. Lin, *Science* 334 (2011) 806; (b) X. Bao, Y. Wang, X. Li, X.-M. Li, Z. Liu, T. Yang, C.F. Wong, J. Zhang, Q. Hao, X.D. Li, *eLife* 3 (2014), e02999.
- [8] (a) W. Wei, X. Liu, J. Chen, S. Gao, L. Lu, H. Zhang, G. Ding, Z. Wang, Z. Chen, T. Shi, J. Li, J. Yu, J. Wong, *Cell Res.* 27 (2017) 898; (b) W. Wei, A. Mao, B. Tang, Q. Zeng, S. Gao, X. Liu, L. Lu, W. Li, J.X. Du, J. Li, J. Wong, L. Liao, *J. Proteome Res.* 16 (2017) 1743.
- [9] (a) T. Komatsu, Y. Urano, *Anal. Sci.* 31 (2015) 257; (b) M. Minoshima, K. Kikuchi, *Anal. Sci.* 31 (2015) 287.
- [10] A.S. Madsen, C.A. Olsen, *Angew. Chem., Int. Ed. Engl.* 51 (2012) 9083.
- [11] (a) S. Mujtaba, L. Zeng, M.M. Zhou, *Oncogene* 26 (2007) 5521; (b) P. Filippakopoulos, S. Picaud, M. Mangos, T. Keates, J.-P. Lambert, D. Barsyte-Lovejoy, I. Felletar, R. Volkmer, S. Müller, T. Pawson, A.-C. Gingras, Cheryl H. Arrowsmith, S. Knapp, *Cell* 149 (2012) 214.
- [12] D. Rooker, Y. Klyubka, R. Gautam, E. Tomat, D. Buccella, *Chembiochem* 19 (2018) 496.
- [13] (a) R. Baba, Y. Hori, S. Mizukami, K. Kikuchi, *J. Am. Chem. Soc.* 134 (2012) 14310; (b) D.R. Rooker, D. Buccella, *Chem. Sci.* 6 (2015) 6456; (c) I.N. Gober, M.L. Waters, *J. Am. Chem. Soc.* 138 (2016) 9452; (d) Y. Xie, J. Ge, H. Lei, B. Peng, H. Zhang, D. Wang, S. Pan, G. Chen, L. Chen, Y. Wang, Q. Hao, S.Q. Yao, H. Sun, *J. Am. Chem. Soc.* 138 (2016) 15596; (e) Y. Xie, L. Chen, R. Wang, J. Wang, J. Li, W. Xu, Y. Li, S.Q. Yao, L. Zhang, Q. Hao, H. Sun, *J. Am. Chem. Soc.* 141 (2019) 18428.
- [14] (a) Q.Q. Li, P.G. Chen, Z.W. Hu, Y. Cao, L.X. Chen, Y.X. Chen, Y.F. Zhao, Y.M. Li, *Chem. Sci.* 8 (2017) 7675; (b) Z.H. Huang, L. Shi, J.W. Ma, Z.Y. Sun, H. Cai, Y.X. Chen, Y.F. Zhao, Y.M. Li, *J. Am. Chem. Soc.* 134 (2012) 8730.
- [15] H. Jiang, S. Khan, Y. Wang, G. Charron, B. He, C. Sebastian, J. Du, R. Kim, E. Ge, R. Mostoslavsky, H.C. Hang, Q. Hao, H. Lin, *Nature* 496 (2013) 110.
- [16] H. Jing, J. Hu, B. He, Y.L. Negrón Abril, J. Stupinski, K. Weiser, M. Carbonaro, Y.-L. Chiang, T. Southard, P. Giannakou, R.S. Weiss, H. Lin, *Canc. Cell* 29 (2016) 297.
- [17] J. Du, Y. Zhou, X. Su, J.J. Yu, S. Khan, H. Jiang, J. Kim, J. Woo, J.H. Kim, B.H. Choi, B. He, W. Chen, S. Zhang, R.A. Cerione, J. Auwerx, Q. Hao, H. Lin, *Science* 334 (2011) 806.